

# SPS IMPEDANCE

E. Métral, G. Arduini, T. Bohl, H. Burkhardt, F. Caspers, H. Damerau, E. Gaxiola, T. Kroyer, H. Medina, G. Rumolo, B. Salvant, E. Shaposhnikova, M. Schokker, J. Tuckmantel (CERN, Geneva, Switzerland), R. Calaga (BNL, Upton, NY, USA) and B. Spataro (INFN, Frascati, Italy)

## Abstract

For many years several measurements of the beam coupling impedance have been performed each year in both longitudinal and transverse planes of the CERN Super Proton Synchrotron to keep track of the evolution of its hardware. Copious types of equipments had to be modified or added in the past to allow the SPS to produce the nominal LHC beam. The next challenge would be the operation of the SPS with higher intensity for the LHC luminosity upgrade, which requires a good knowledge of the machine impedance and in particular of its major contributors. The current understanding of the measurements performed over the last few years is presented in this paper. In particular, this analysis reveals that the longitudinal impedance is reasonably well understood, while the situation is less satisfactory in the transverse planes, where about half of the measured impedance still needs to be identified.

## INTRODUCTION

Before 2001, the longitudinal single bunch (microwave) instability has been observed in the SPS in practically all operation modes: with leptons and protons, below and above transition energy, with RF on and RF off [1,2]. Even though in most cases the associated longitudinal emittance blow-up was not detrimental, it became a significant issue for the high-brightness beams required for LHC. Different solutions to avoid or cope with the uncontrolled emittance blow-up due to the microwave instability were studied. The most attractive cure was the removal or shielding of the elements concerned [3]. Different types of reference measurements were initiated in order to followup the impedance reduction program and to see the consequences on the beam. The global effect of the SPS impedance reduction in the longitudinal plane can be observed in Fig. 1, where the reference measurements done in 1999 (before impedance reduction) are compared to 2001 (after). Note that two mechanisms are expected to lead to an increase of the bunch length with intensity; firstly the potential-well distortion defined by the inductive part of the effective (i.e. taking into account the bunch spectrum) longitudinal impedance  $\text{Im}[Z_l/n]_{\text{eff}}$  and then, above some threshold intensity the uncontrolled emittance blow-up induced by the microwave instability. The difference in the slopes of Fig. 1 is around a factor 7. It can also be concluded that in 1999 the microwave instability threshold was at or below  $3 \times 10^{10}$  p/b. In 2001 the smooth

increase with intensity due to potential-well distortion can clearly be observed. Simulations showed that the impedance of the vacuum pumping ports was responsible for most of the uncontrolled emittance blow-up observed before 2001. The shielding of these elements ( $\sim 1000$  vacuum pumping ports) eliminated the microwave instability. Note that in addition several kickers were also removed (the total number of kickers in 2001 was 11) as well as the lepton RF cavities. It was deduced from measurements (as will be seen also later in this paper) that the impedance reduction factor was  $\sim 2.5$  in the longitudinal plane, whereas it was only  $\sim 0.4$  in the vertical one.

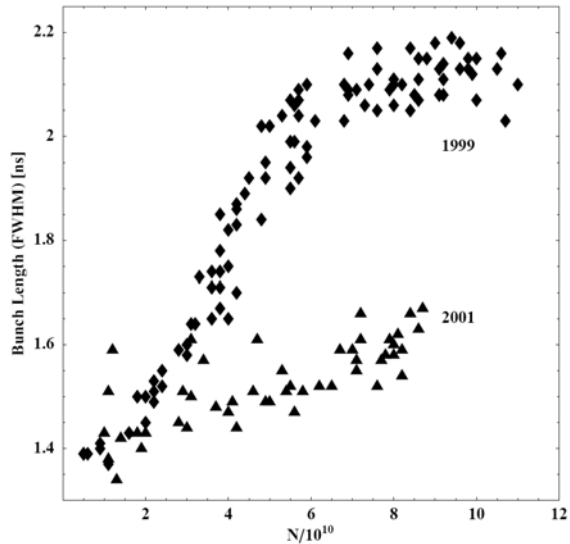


Figure 1: Bunch length measured 600 ms after injection as a function of bunch intensity in 1999 and 2001. Data taken at 26 GeV/c, with the RF voltage  $V_{\text{RF}} = 900$  kV and the longitudinal emittance  $\varepsilon_L = 0.15$  eVs [1].

To extract the beam towards the LHC, new extraction kickers (MKE) were required. In 2003, the first 5 MKE kickers (out of 9 in total) were installed in the sextant LSS4 (i.e. 16 kickers in total were present in the SPS). In 2006, the remaining 4 MKE kickers were added in sextant LSS6 (leading to a total of 20 kickers). Note that one of the MKE kicker was shielded on 2 cells. Finally, in 2007 one MKE kicker was removed and one MKE was “fully” shielded, leading to a total of 19 kickers. To be able to follow the impedance increase and to see the consequences for the beam, the same reference measurements had been continued. In parallel a lot of

work was devoted to estimate better the resistive-wall impedance [4] and the results were applied to the MKE kickers and compared to bench measurements (see later).

Detailed measurements were also performed in 2003 in the SPS right after injection at 26 GeV/c, where a fast single-bunch vertical instability develops when the longitudinal emittance of the beam is too small [5]. Figure 2 is an example of what was observed with a high-intensity single bunch ( $\sim 1.2 \times 10^{11}$  p/b) of low longitudinal emittance ( $\sim 0.2$  eVs). The RF voltage was  $V_{RF} \approx 600$  kV, which corresponds to the synchrotron period  $T_s = 7.1$  ms. Keeping the chromaticity close to zero, the bunch was stabilized when the intensity was reduced to  $\sim 6 \times 10^{10}$  p/b. A detailed comparison between the measurements and HEADTAIL [6] simulations was performed in the past. As can be seen in Fig. 3, a good agreement between the two was already revealed when the measured “equivalent” broad-band impedance model (with a shunt impedance  $R_y = 20$  M $\Omega$ /m, a resonance frequency  $f_r = 1$  GHz and a quality factor  $Q = 1$ ) was used. In particular the analysis in the time domain revealed a travelling-wave pattern along the bunch, which is believed to be the signature of a transverse-mode coupling instability (the coupling of standing-wave patterns leads to a travelling wave). After having analysed the instability in the time domain, the next step consisted to analyse the instability in the frequency domain to try and observe a coupling between the azimuthal modes. A sensitive frequency analysis of the HEADTAIL simulations output was therefore done using SUSSIX [7], which brought to light the fine structure of the mode spectrum of the bunch coherent motion. A coupling between the azimuthal modes -2 and -3 was clearly observed to be the reason for this fast instability, which was in good agreement with the predictions from MOSES [8] for the case of a round geometry (see Fig. 4) [9]. The next steps consisted then on one hand to improve the model of the SPS transverse (vertical) impedance to make more realistic predictions from theory and/or HEADTAIL simulations and on the other hand to try and measure the mode coupling. The first step was started adding the computed contributions from all the kickers plus several other elements, and is discussed later in the present paper, whereas the measurements still have to be analysed in detail.

In addition to coherent instabilities, the real part of the longitudinal impedance of the ferrites installed in the MKE extraction kickers lead to significant beam-induced heating of the magnets. The temperature variation is usually measured on the ceramic spacers, which touch the ferrites. If a part of the ferrite itself happens to reach temperatures above the Curie temperature, around 125°C, it loses its magnetic properties and the magnetic field strength is reduced. Structural damage to the kicker magnets cannot be excluded for temperatures above 150°C. Presently the beam in the SPS is aborted if the

measured MKE temperature reaches 90°C.

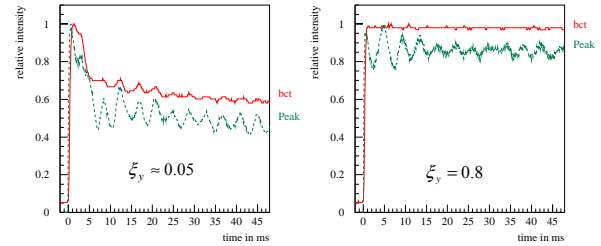


Figure 2: Measured relative (normalized to the value at injection) bunch intensity vs. time in the SPS machine in 2003. bet stands for beam current transformer and Peak stands for peak intensity. The bunch, which is unstable when  $\xi_y \approx 0.05$  (left) is stabilized by increasing the (relative) chromaticity to  $\xi_y = 0.8$  (right).

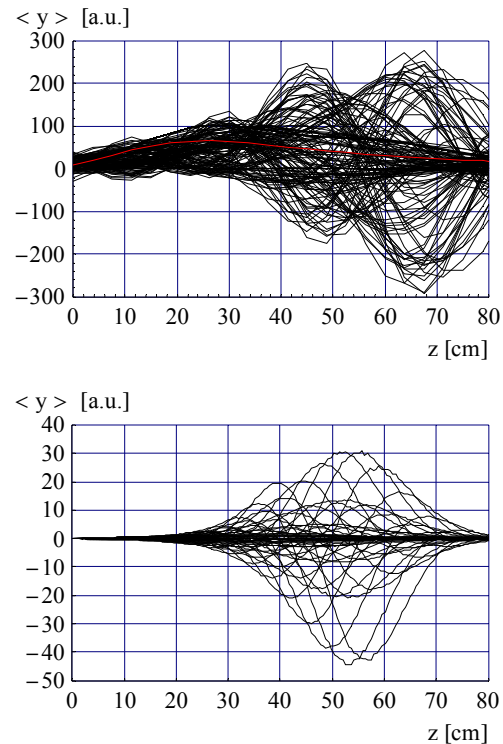


Figure 3: (Upper) Measured evolution of the vertical centroid position along the bunch  $\langle y \rangle = N(z) \times y_{av}(z)$ , where  $N(z)$  is the longitudinal bunch profile, using the “Head-Tail” monitor [10] (with the traces of all the 150 turns superimposed), for a vertical (relative) chromaticity close to zero (see Fig. 2). The first turn after injection is shown in red. The head of the bunch (truncated at  $\pm 2\sigma_z$ ) is on the left and the tail on the right. (Lower) Simulated evolution of the vertical centroid position along the bunch using the HEADTAIL code (with the traces of all the turns superimposed). The head of the bunch (truncated at  $\pm 2\sigma_z$ ) is on the left.

The outline of the present paper is the following: the first section deals with the resistive-wall formula used to estimate the impedance of all the SPS kickers. The second section is devoted to the detailed comparison between measurements and theoretical predictions. Finally, new HEADTAIL simulations in the longitudinal plane are discussed.

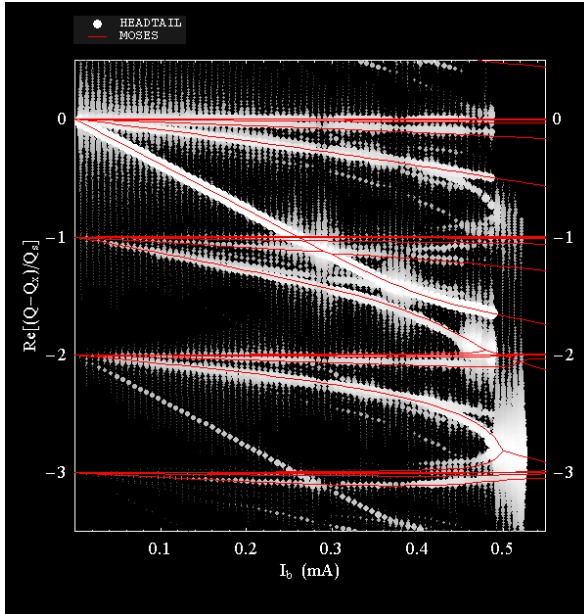


Figure 4: Head-tail modes vs. bunch intensity for  $\epsilon_L = 0.2$  eVs,  $\sigma_t = 0.67$  ns,  $V_{RF} = 600$  kV and  $\xi_x = 0$ . MOSES (red lines) vs. HEADTAIL (white dots) results analyzed with SUSSIX. The impedance used here is a broad-band impedance with a shunt impedance  $R_y = 10$  M $\Omega$ /m (instead of 20 M $\Omega$ /m above), a resonance frequency  $f_r = 1$  GHz and a quality factor  $Q = 1$ .

### RESISTIVE-WALL IMPEDANCE OF THE MKE KICKERS

Figure 5 shows the real cross-section of a MKE magnet. From the impedance point of view, it can be

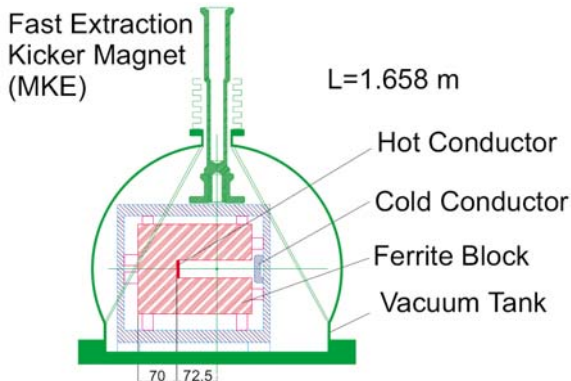


Figure 5: Cross-section of a MKE magnet.

approximated by the simpler geometry of Fig. 6. Detailed analytical studies revealed that for the computation of the transverse (vertical) impedance, the model of two infinite ferrite plates is well justified and Zotter's formula [4] should be used, as confirmed by measurements shown in Fig. 7. However, for the computation of the longitudinal impedance, it is mandatory to take into account the perfect conductor on both sides (left and right) and use Tsutsui's formula [11]. This was confirmed by measurements [12] as can be seen in Figs. 8 and 9. To get rid of the operational issue of the heating associated with the real part of the longitudinal impedance of the MKE kickers, it was suggested to print conducting strips directly onto the ferrite. This was done on the kicker MKE-L10 (see Fig. 10) and the effect on the impedance was measured (see Fig. 11). A more detailed description of the impedance measurements and of the approaches to reduce kicker heating can be found in Ref. [13]. It can be concluded from Fig. 11 that the real part of the impedance is indeed considerably reduced, even though resonances are created near 50 MHz and 1.7 GHz.

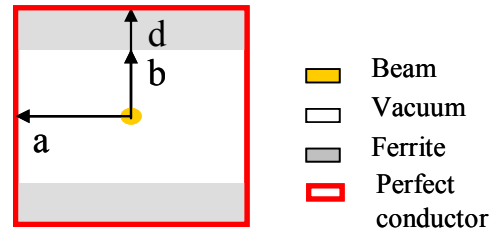


Figure 6: Simplified model for the computation of the MKE kicker impedance.

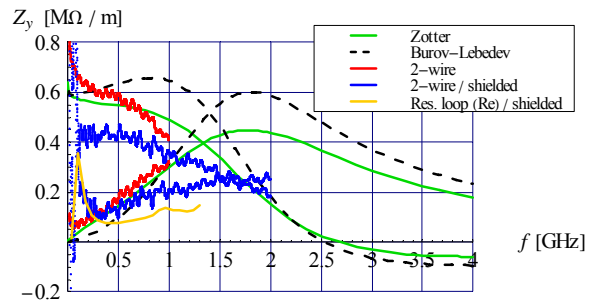


Figure 7: Measurement (with 2 wires, in red) of both real and imaginary parts of the vertical impedance of an SPS kicker vs. frequency, compared to Zotter's [4] (in green) and Burov-Lebedev's [14] (in black) theories. The blue and yellow curves correspond to two different methods (with 2 wires and resonant loop) of measurement in the case of a "shielded" kicker with printed strips used to mainly reduce the real part of the longitudinal impedance and the associated heating (see Figs. 10 and 11).

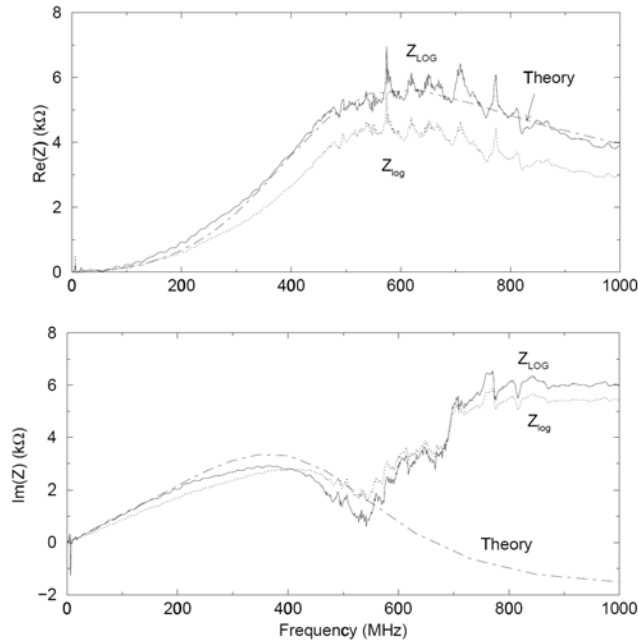


Figure 8: Measurement of the real (upper) and imaginary (lower) part of the longitudinal impedance of a SPS MKE kicker vs. frequency in 2000, compared to Tsutsui's theory [11]. The increase in the imaginary part after  $\sim 500$  MHz was then understood as can be seen in Fig. 9.

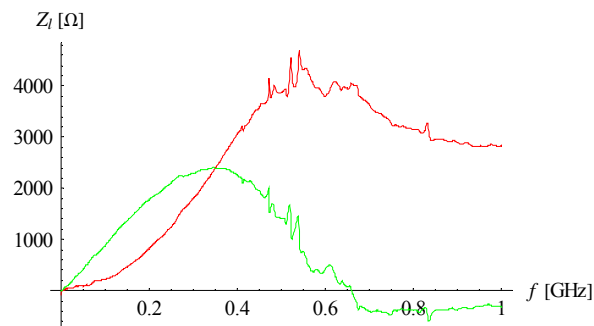


Figure 9: Measurement of the real (red) and imaginary (green) part of a SPS MKE kicker impedance vs. frequency in 2006.

In fact two resonances were also introduced below 100 MHz in the transverse plane (barely visible in Fig. 7). The effects of these resonances were studied both in the longitudinal and transverse planes, and it was concluded that they were not too harmful and that the impedance reduction campaign for the MKE kickers should be pursued by the deposition of conducting strips as this has a significant impact on the overall longitudinal impedance and on the kicker heating [15].

It was concluded from the above comparisons between analytical formulae and measurements of both longitudinal and transverse impedances that our

theoretical estimates are quite satisfactory and that one could use them to estimate both longitudinal and transverse resistive-wall impedances of all the SPS kickers in the past few years. These estimates are compared to beam-based measurements in the next section.



Figure 10: Printed conducting strips directly on top of the ferrite of the MKE-L10 kicker.

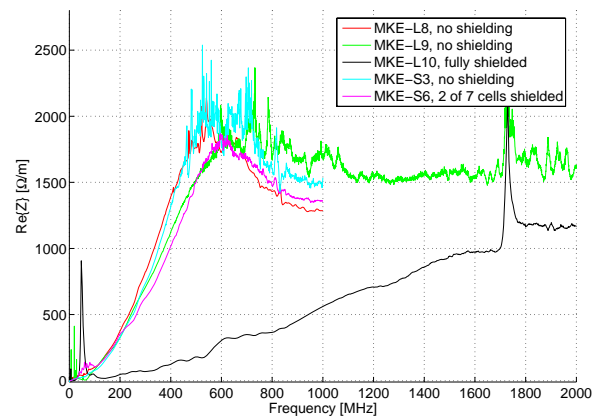


Figure 11: Measurement of the real part of the longitudinal impedance of different SPS MKE kickers vs. frequency, and in particular for the MKE-L10 (in black) fully equipped with printed strips to reduce the real part of the longitudinal impedance.

## MEASUREMENT VS. THEORY

### *Transverse Coherent Tune Shift vs. Intensity*

The measurements of the single-bunch transverse (vertical) coherent tune shift vs. intensity [16] over the last few years are depicted in Fig. 12 [17]. It can be first seen that in 2001 the measured “total” (i.e. dipolar plus quadrupolar [18]) effective impedance was reduced by 40% compared to the measured value in 2000 (as already mentioned in Introduction). Secondly, one can observe that the measured “total” impedance increase from 2001

to 2006 (i.e. due to the installation of the 9 MKE kickers) is  $4.5 \text{ M}\Omega/\text{m}$ , which has to be compared to  $5.2 \text{ M}\Omega/\text{m}$  expected from theory (see Table 1). Furthermore, a slight reduction of the impedance was expected in 2007 (due to the removal of one MKE kicker and shielding of another one). This seems also to be reflected in Fig. 12, even though one might reach the precision limit for the measurements and the exact predicted “total” impedance of the shielded kicker could not be given as the quadrupolar impedance is missing (only the dipolar impedance was measured in Fig. 7). This good agreement reveals that the impact of the hardware modifications can be well explained since 2001. Note that the imaginary part of the vertical effective dipolar impedance of the shielded kicker is  $\text{Im}[Z_{y,\text{dip}}]_{\text{eff}} = 0.24 \text{ M}\Omega/\text{m}$ , whereas it was  $0.27 \text{ M}\Omega/\text{m}$  before the shielding, revealing a small effect of the shielding in the vertical plane. Furthermore, the imaginary part of the vertical effective “total” impedance from space charge (which contributes to the coherent tune shift) is  $\text{Im}[Z_y]_{\text{eff}} = 2.6 \text{ M}\Omega/\text{m}$  (it is  $0.04 \text{ M}\Omega/\text{m}$  in the horizontal plane).

The conclusions of these measurements are that (i) the contribution from all the kickers vs. time can be reasonably well explained, (ii) all the kickers in 2006 (and 2007) contribute to  $\sim 40 \%$  of the total measured impedance and (iii)  $13 \text{ M}\Omega/\text{m}$  ( $= 19.1 - 3.5 - 2.6$ ) are still missing (already in 2001).

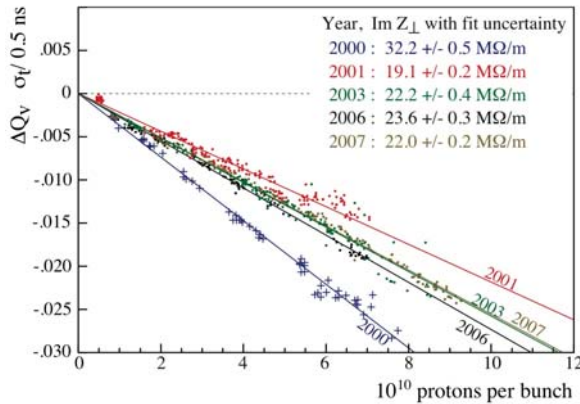


Figure 12: Measurements of the single-bunch vertical coherent tune shift vs. intensity over the last years [17].

Table 1: Summary and comparison between beam-based measurements (of the whole SPS ring) and theoretical predictions (considering only the contribution from all the kickers).

| $\text{Im}(Z_y)_{\text{eff}}$ [ $\text{M}\Omega/\text{m}$ ] | Meas | delta | Theory (kickers) | delta | Error delta [%] |
|---|------|-------|------------------|-------|-----------------|
| 2001  | 19.1 |       | 3.5              |       |                 |
| 2003  | 22.2 | 3.1   | 6.4              | 2.9   | 7               |
| 2006  | 23.6 | 1.4   | 8.7              | 2.3   | -39             |
| 2007  | 22   | -1.6  |                  |       |                 |

### Fast Vertical Single-Bunch Instability Intensity Threshold at Injection

Taking into the contribution from all the (20) kickers in 2006, the vertical wake field has been obtained through ZBASE3 (which is a new version still under development of the impedance database ZBASE [19]). It is plotted in Fig. 13 together with the wake field of the broad-band resonator model ( $10 \text{ M}\Omega/\text{m}$ ) used for the transverse mode coupling analysis (see Fig. 4). The HEADTAIL simulation code has been upgraded to be able to read the wake field from a table of data instead of using an analytical formula, and the result from the HEADTAIL simulations is depicted in Fig. 14. It reveals that the intensity threshold found with the same bunch parameters as above and the “real” (computed) impedance from all the (20) kickers in 2006 is  $N_b^{\text{th}} \approx 1.1 \times 10^{11}$  p/b. In order to check that the results obtained with the recently upgraded

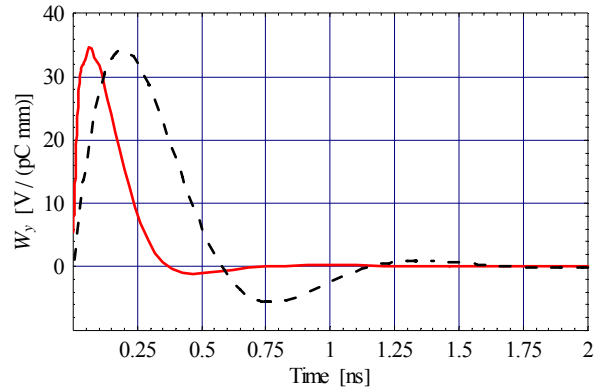


Figure 13: Theoretical wake field from all the (20) SPS kickers in 2006 (red curve) compared to the one from the broad-band resonator model ( $10 \text{ M}\Omega/\text{m}$ ) used for the transverse mode coupling analysis (see Fig. 4) (dashed black curve).

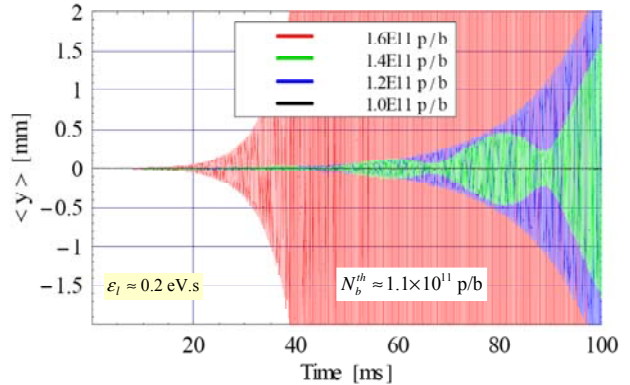


Figure 14: Evolution of the vertical centroid position (simulated with the HEADTAIL code) vs. time using the “real” computed wake field for all the (20) SPS kickers in 2006 (see Fig. 13). In the legend the numbers refer to the number of protons per bunch.

HEADTAIL code are correct, the wake field of Fig. 13 has been fitted by a broad-band resonator model (see Fig. 15) and the latter has been used to perform MOSES computation (see Fig. 16). The fitted resonator has a shunt impedance of 3.5 MΩ/m, a resonance frequency of 2.3 GHz and a quality factor of 0.6. As can be seen from

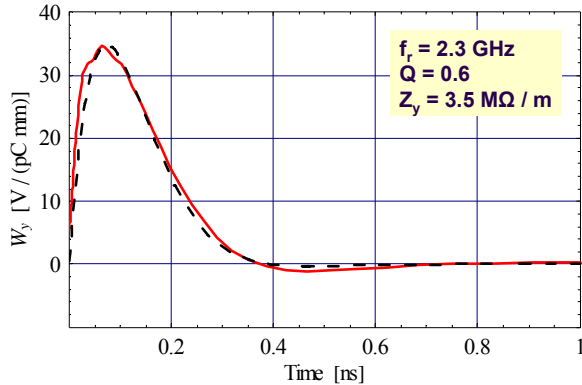


Figure 15: Fit (dashed black curve) of the wake field for all the (20) SPS kickers in 2006 (red curve).

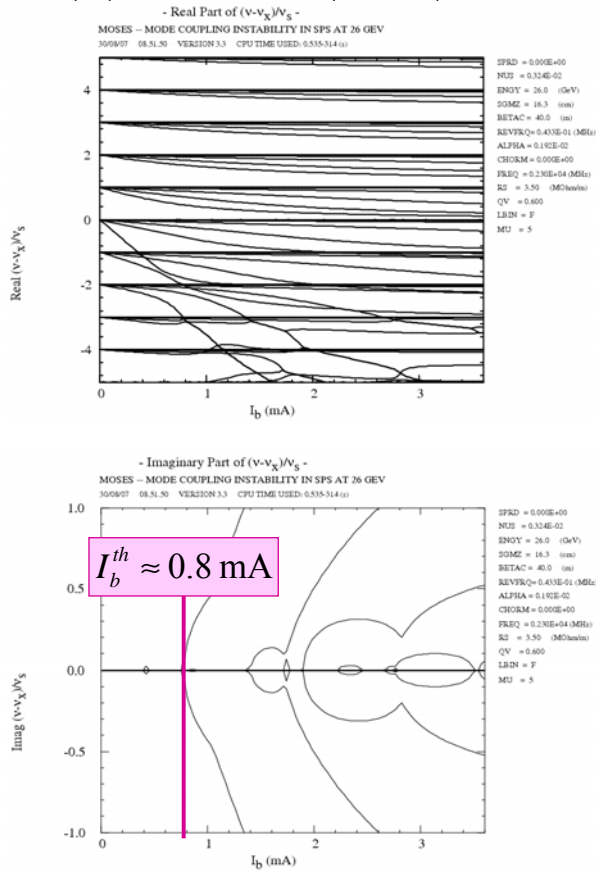


Figure 16: MOSES computation with the fitted resonator of Fig. 15. Real (upper) and imaginary (lower) parts of the normalised vertical tune shift vs. bunch intensity.

Fig. 16 (lower) the intensity threshold is  $I_b^{th} \approx 0.8$  mA, which corresponds to a threshold in the number of protons per bunch of  $N_b^{th} \approx 1.15 \times 10^{11}$  p/b. This value is therefore in very good agreement with the one previously found with HEADTAIL ( $\sim 1.1 \times 10^{11}$  p/b), which constitutes a satisfactory benchmark between the two codes.

The conclusion from these measurements is that predicted intensity threshold with the “real” computed wake field from all the (20) kickers in 2006 is about a factor 2 higher ( $\sim 1.1 \times 10^{11}$  p/b predicted compared to  $\sim 0.6 \times 10^{11}$  p/b measured). Here again, this means that the contribution from the kickers to the vertical impedance is only  $\sim 50\%$ .

### Head-Tail Growth/Decay Rate

Changing the (vertical) chromaticity the growth or decay rates of the single-bunch head-tail instability (which depend only on the dipolar impedance) can be measured. This provides information about the real part of the vertical (dipolar) impedance. Using the fit of the “real” computed wake field for all the (20) SPS kickers in 2006 discussed in the previous section, the predicted head-tail growth/decay rates are compared to the measured ones in Fig. 17.

The conclusion from these measurements is also that the real part of the effective vertical impedance from all the (20) kickers in 2006 contribute to  $\sim 50\%$  of the total measured impedance. Therefore, the three measurements of the vertical impedance are quite consistent.

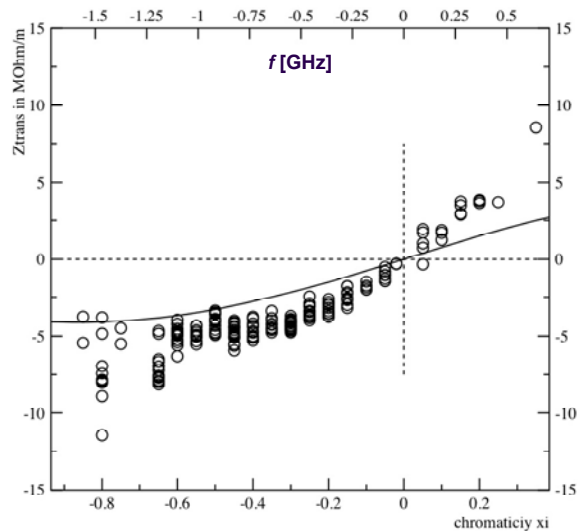


Figure 17: Comparison between the measured (dots) and computed (full black curve) real part of the effective vertical impedance vs. chromaticity. The computation was made using the fitted resonator for 2006, i.e. with a shunt impedance of 3.5 MΩ/m, a resonance frequency of 2.3 GHz and a quality factor of 0.6.

### Quadrupole Oscillation Frequency Shift vs. Intensity

The inductive part of the effective longitudinal impedance can be assessed by measuring the quadrupole oscillation frequency shift vs. intensity. The results of these measurements over the last years can be found in Fig. 18 [20]. These estimates were based on the analysis of the data of Fig. 19. It can be first seen that in 2001 the measured effective impedance was reduced by a factor of  $\sim 2.5$  compared to the measured value in 1999 (as already mentioned in Introduction). Secondly, one can observe that the effective impedance increase from 2001 to 2006 (i.e. due to the installation of the 9 MKE kickers) is  $3 \Omega$ , which has to be compared to  $4 \Omega$  expected from theory (see Table 2). The agreement is quite good if one keeps also in mind that these measurements are very sensitive to the bunch length (see Appendix E). Finally, a slight reduction of the impedance was expected in 2007 (due to the removal of one MKE kicker and shielding of another one). As can be seen in Figs. 18 and 19, contrary to the expectations, an increase of the impedance by  $\sim 40\%$  was observed. This issue still has to be investigated in detail. More measurements are planned at the end of the 2007 run to try and understand the reason of this unexpected and significant increase. Note that the longitudinal effective inductive impedance of the shielded kicker is  $\text{Im}[Z_{\perp/n}]_{\text{eff}} = 0.1 \Omega$ , whereas it was  $0.4 \Omega$  before the shielding, which reveals the important effect of the shielding. Furthermore, the longitudinal effective inductive impedance from space charge (which contributes to the frequency shift) is  $\text{Im}[Z_{\perp/n}]_{\text{eff}} \approx -1 \Omega$ , and it has already been subtracted from the above cited numbers (unlike the transverse plane).

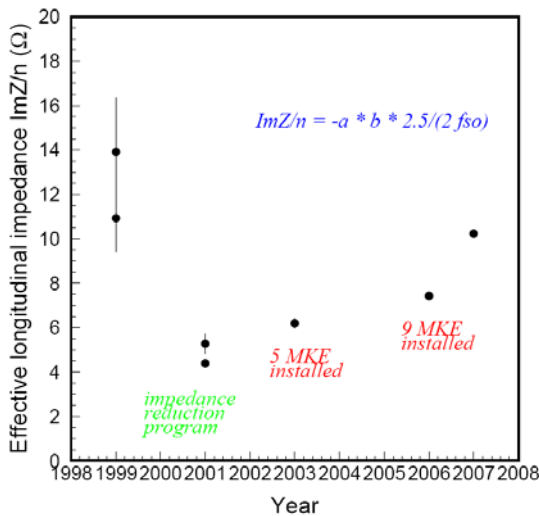


Figure 18: Longitudinal effective inductive impedance as deduced from the quadrupole oscillation frequency shift over the last few years (see Fig. 19).

The conclusions from these measurements are that (i) the contribution from all the kickers vs. time can be reasonably well explained until 2006, (ii) an increase by  $\sim 40\%$  was observed in 2007, which is not explained yet as a slight reduction was predicted.

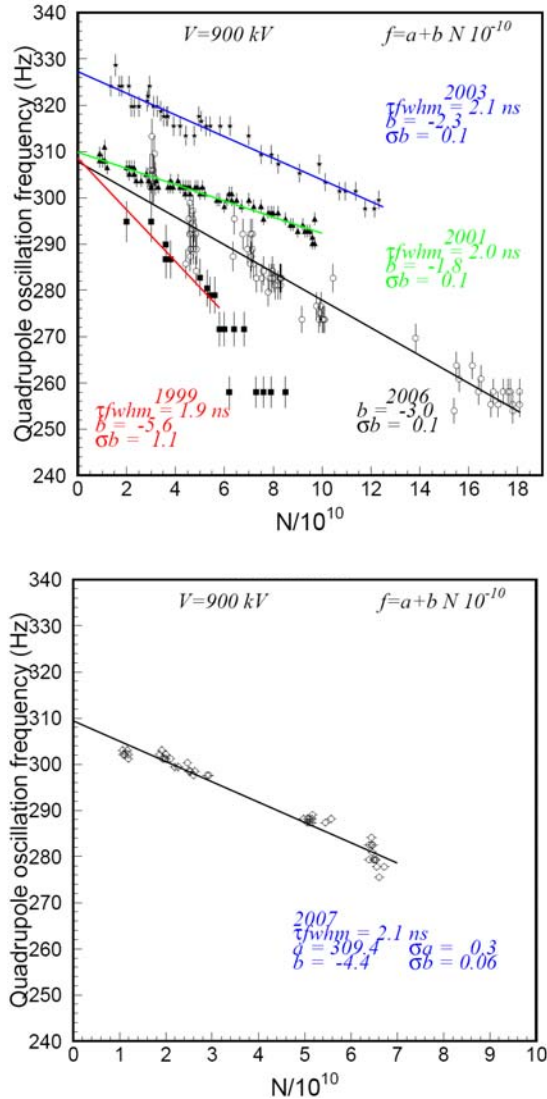


Figure 19: Quadrupole oscillation frequency vs. intensity from 1999 to 2006 (upper), and in 2007 (lower).

Table 2: Summary and comparison between beam-based measurements (of the whole SPS ring) and theoretical predictions (considering only the contribution from all the kickers).

| $\text{Im}(Z_{\perp/n})_{\text{eff}} [\Omega]$ | Meas | delta | Theory (kickers) | delta | Error delta [%] |
|--|------|-------|------------------|-------|-----------------|
| 2001   | 4.4  |       | 1.2              |       |                 |
| 2003   | 6.2  | 1.8   | 3.4              | 2.2   | -18             |
| 2006   | 7.4  | 1.2   | 5.2              | 1.8   | -33             |
| 2007   | 10.2 | 2.8   | 4.4              | -0.8  | -450            |

## Power Loss

All the measurements discussed above used the same kind of beam: a single bunch with low longitudinal and transverse emittances (compared to the nominal LHC bunches). Considering now the nominal LHC beam in the SPS, i.e. 4 batches of 72 bunches with  $1.2 \times 10^{11}$  p/b and an rms bunch length of 0.7 ns, yields the power losses shown in Table 3 over the last years. Note that the power loss for the shielded kicker is computed to be 407 W, whereas it is expected to be 1127 W without the shielding. This means that a reduction in the power loss by a factor of  $\sim 3$  is predicted. This was confirmed by measurements as a reduction by a factor 3-4 was observed [21].

Table 3: Power loss computed with a nominal LHC beam in the SPS (4 batches of 72 bunches with  $1.2 \times 10^{11}$  p/b and an rms bunch length of 0.7 ns).

| Power loss [W] | Theory | delta |
|----------------|--------|-------|
| 2001           | 2085   |       |
| 2003           | 8027   | 5942  |
| 2006           | 12742  | 4715  |
| 2007           | 10792  | -1950 |

## HEADTAIL SIMULATIONS IN THE LONGITUDINAL PLANE

As the longitudinal impedance was measured to have increased by  $\sim 40\%$  in 2007, HEADTAIL simulations were performed in the longitudinal plane to see where the longitudinal microwave intensity threshold stands. A modelled resonator impedance was first used with a shunt impedance of  $10 \Omega$  (as deduced from Table 2), a resonance frequency of 1 GHz and a quality factor of 1. The bunch parameters were taken to be the same as the ones used for the transverse mode coupling analysis. The rms bunch length vs. intensity is plotted in Fig. 20, where

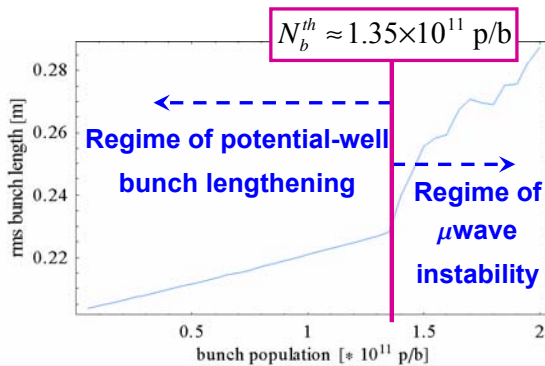


Figure 20: Rms bunch length vs. intensity simulated with the HEADTAIL simulation code. The same parameters as the ones for the transverse mode coupling analysis were used. A modelled resonator impedance was used with a shunt impedance of  $10 \Omega$  (as deduced from Table 2), a resonance frequency of 1 GHz and a quality factor of 1.

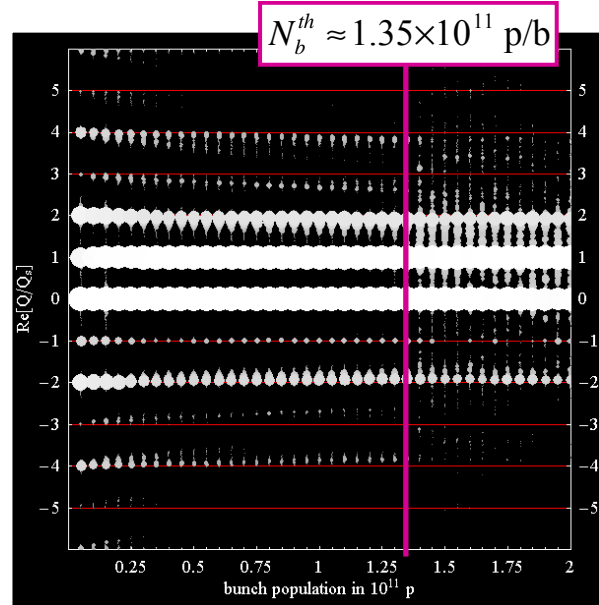


Figure 21: Longitudinal modes vs. bunch intensity for the same bunch parameters as the ones used in the transverse mode coupling analysis. However, the impedance used here is a modelled broad-band impedance with a shunt impedance of  $10 \Omega$  (see Table 2), a resonance frequency of 1 GHz and a quality factor of 1.

two regimes can be clearly distinguished. The first (almost) linear one corresponds to the potential-well bunch lengthening regime. The second is the regime of microwave instability. On this picture the intensity threshold can be deduced unambiguously and is  $N_b^{\text{th}} \approx 1.35 \times 10^{11}$  p/b. Applying the same sensitive frequency analysis as was done previously for the transverse plane (with SUSSIX) of the HEADTAIL simulations output, the evolution of the longitudinal coherent frequency shifts vs. intensity is depicted in Fig. 21. No clear mode coupling as in the transverse plane is observed, which may be due to the fact that the frequency signals are largely dominated by the modes 0 and 1. However, close to the intensity threshold some activity can be seen around mode 2 (with modes 1 and 3), and this will be investigated in detail in the future.

To check the validity of the analytical formula for the prediction of the potential-well bunch lengthening, the longitudinal effective inductive impedance was deduced from the slope of Fig. 20, and compared to the known impedance introduced in HEADTAIL. From the usual 4<sup>th</sup> order equation [22], a simplified equation can be deduced in our case and is given by

$$\text{Im} \left[ \frac{Z_l}{n} \right]_{\text{protons}} \approx - \frac{4 \cos \phi_s \pi^2 V_{\text{RF}} h (f_0 \tau_{b0})^2}{3 e} \times \frac{d \tau_b}{d N_b}, \quad (1)$$

where  $\phi_s$  is the RF phase of the synchronous particle ( $\cos\phi_s > 0$  below transition and  $\cos\phi_s < 0$  above),  $V_{RF}$  the peak RF voltage,  $h$  the harmonic number,  $f_0$  the revolution frequency,  $\tau_b$  the total bunch length in seconds (with  $\tau_{b0}$  the value at zero intensity) and  $e$  the elementary charge. Applying Eq. (1) to the slope of Fig. 20 yields  $\text{Im}[Z_l/n]_{\text{eff}} \approx 8.4 \Omega$ , whereas  $10 \Omega$  were used in HEADTAIL, which is in good agreement (the error is 16%).

The intensity threshold of the microwave instability has also been compared to the analytical formula of Ref. [23] given by

$$\frac{|Z_l^{BB}/n|}{1.2} \times \left[ 1 - \text{Sgn}(\eta) \times \frac{3}{4} \left( \frac{|Z_l^{SC}/n|}{|Z_l^{BB}/n|} - 1 \right) \right]^{1/4} \quad (2)$$

$$\leq \frac{(E/e)\beta^2|\eta|}{I_{p0}} \times \left( \frac{\Delta p}{p_0} \right)_{\text{FWHH},0}^2,$$

where BB stands for Broad-Band and SC for Space Charge impedance,  $\eta = \gamma_{tr}^{-2} - \gamma^{-2} = (\Delta T/T_0)/(\Delta p/p_0)$  is the slippage factor,  $\text{Sgn}(\eta)$  denotes the sign of  $\eta$  (it is - below transition and + above),  $\beta$  is the relativistic velocity factor,  $E$  the total beam energy,  $I_{p0} = 3 e N_b / (2 \tau_{b0})$  is the bunch peak current (without potential-well distortion) considering a parabolic line density, and  $(\Delta p/p_0)_{\text{FWHH},0}$  is the full width at half height of the relative momentum spread (without potential-well distortion). Note that in the present case,

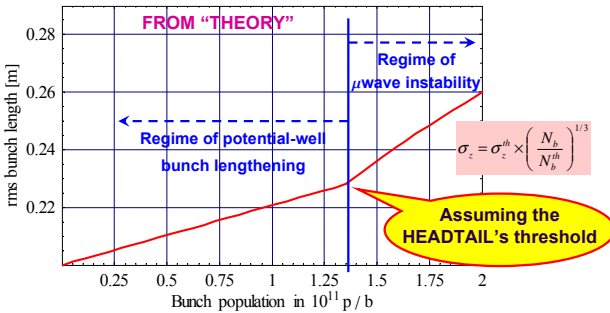


Figure 22: Rms bunch length variation vs. intensity as predicted from theory [22].

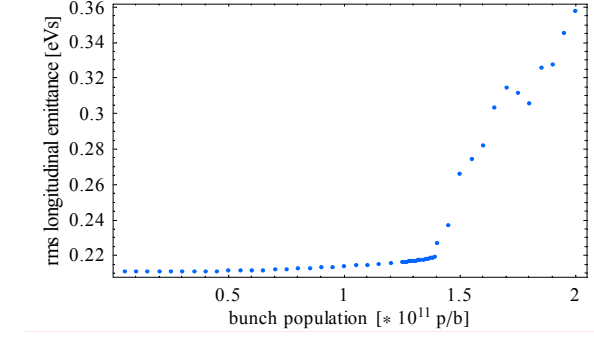
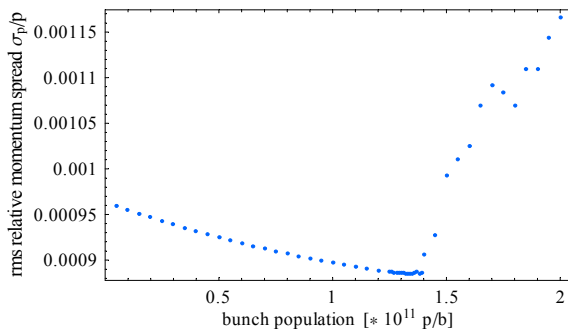


Figure 23: Rms relative momentum spread (upper) and rms longitudinal emittance (lower) vs. intensity from HEADTAIL simulations.

i.e. above transition and without space charge, Eq. (2) leads to the same result as the usual Keil-Schnell-Boussard approximation. Applying Eq. (2) yields  $N_b^{\text{th}} \approx 0.7 \times 10^{11}$  p/b, i.e. the theoretical prediction is about a factor 2 lower than the simulated one ( $N_b^{\text{th}} \approx 1.35 \times 10^{11}$  p/b). Furthermore, in the microwave instability regime the bunch length was estimated in Ref. [22] to vary with the power 1/3 of the intensity, which seems to underestimate the effect (see Fig. 22 from theory compared to measurements in Fig. 20). For completeness the evolution of both momentum spread and longitudinal emittance vs. intensity obtained from HEADTAIL is shown in Fig. 23.

The next steps would consist to improve the model of the SPS longitudinal impedance to make more realistic predictions from theory and/or HEADTAIL simulations and to try and measure the (possible) mode coupling.

## CONCLUSION

All the comparisons performed so far between transverse analytical estimates and measurements of the effective impedance are in good agreement over the last few years, when relative values are discussed. All the kickers can only explain  $\sim 40\%$  of the measured vertical impedance. Removing the contribution from space charge to the coherent tune shift,  $13 \text{ M}\Omega/\text{m}$  are still unexplained. In addition to the kickers, the impedance of several other equipments has been computed or simulated, such as the 108 horizontal and vertical beam position monitors,  $\sim 1000$  (shielded) vacuum pumping ports, the four Travelling-Wave (TW) 200 MHz cavities and the high-energy beam dump absorber (See Appendices). However, their contribution cannot explain the missing  $13 \text{ M}\Omega/\text{m}$ . The next step will therefore consist in identifying additional sources of impedance.

In the longitudinal plane, the situation is different. Here again a good agreement between measurements and theory is obtained when relative values are mentioned (i.e. for the contribution from all the kickers). Furthermore, it seems that even for the absolute value the

agreement is relatively good as the main remaining part,  $\sim 3.2 \Omega$  ( $= 4.4 \Omega - 1.2 \Omega$ ) in 2001, could be mainly explained by the four TW 200 MHz cavities, whose inductive effective longitudinal impedance is predicted to be very close to this value (see Appendix F). This study still has to be finalized and the exact contribution from the other (800 MHz) RF system has to be computed. However, one major issue remains in our understanding: why did the longitudinal effective impedance measured in 2007 increase by  $\sim 40\%$  compared to 2006, whereas a slight reduction was foreseen?

### REFERENCES

- [1] T. Bohl et al., "Impedance Reduction in the CERN SPS as seen from Longitudinal Beam Measurements", Proc. EPAC2002, Paris, France.
- [2] LHC Design Report, CERN-2004-003, Chap. 17.
- [3] P. Collier et al., "Reducing the SPS Machine Impedance", Proc. EPAC2002, Paris, France.
- [4] E. Métral et al., "Resistive-Wall Impedance of an Infinitely Long Multi-Layer Cylindrical Beam Pipe", Proc. PAC2007, Albuquerque, New Mexico, USA, June 25-29, 2007.
- [5] G. Arduini et al., "Observation of a Fast Single-Bunch Transverse Instability on Protons in the SPS", Proc. EPAC'04, Lucerne, Switzerland, 2004.
- [6] G. Rumolo and F. Zimmermann, "Practical user guide for HEADTAIL", CERN-SL-Note-2002-036 AP.
- [7] R. Bartolini and F. Schmidt, "SUSSIX : A Computer Code for Frequency Analysis of Non-Linear Betatron Motion", CERN SL/Note 98-017 (AP) updated June 29, 1998.
- [8] Y. H. Chin, "User's guide for new MOSES version 2.0: MOde-coupling Single bunch instability in an Electron Storage ring", CERN/LEP-TH/88-05, 1988.
- [9] B. Salvant et al., "Transverse Mode Coupling Instability in the SPS: HEADTAIL simulations and MOSES computations", these proceedings.
- [10] D. Cocq et al., "The Measurement of Chromaticity via a Head-Tail Phase Shift" presented at BIW'98, Stanford, CA, USA, May 1998.
- [11] H. Tsutsui, "Some Simplified Models of Ferrite Kicker Magnet for Calculation of Longitudinal Coupling Impedance", CERN-SL-2000-004 AP.
- [12] F. Caspers et al., "Impedance Evaluation of the SPS MKE Kicker with Transition Pieces between Tank and Kicker Module", CERN-SL-2000-071 (AP).
- [13] T. Kroyer et al., "Longitudinal and Transverse Wire Measurements for the Evaluation of Impedance Reduction Measures on the MKE Extraction Kickers", CERN-AB-Note-2007-028.
- [14] A. Burov and V. Lebedev, "Transverse Resistive Wall Impedance for Multi-Layer Flat Chambers", Proc. of EPAC 2002, Paris, France.
- [15] CERN APC meetings held on 27/04/2007 and 11/05/2007 (<http://ab-div.web.cern.ch/ab-div/Meetings/APC/Welcome.html>).
- [16] H. Burkhardt et al., "Coherent Beam Oscillations and Transverse Impedance in the SPS", Proc. of EPAC 2002, Paris, France.
- [17] H. Burkhardt, CERN APC meeting held on 17/08/07 (<http://ab-div.web.cern.ch/ab-div/Meetings/APC/Welcome.html>).
- [18] A. Burov and V. Danilov, Phys. Rev. Lett. **82**, 2286-2289 (1999).
- [19] O. Bruning, "ZBASE user's guide Version 1.1: an Impedance Data Base Program", CERN-SL-96-069-AP.
- [20] E. Shaposhnikova, CERN APC meetings held on 11/05/07 and 03/08/07 (<http://ab-div.web.cern.ch/ab-div/Meetings/APC/Welcome.html>).
- [21] L. Ducimetière, private communication (2007).
- [22] J.L. Laclare, "Bunched Beam Coherent Instabilities", CERN Accelerator School, CERN 87-03, p. 264.
- [23] E. Métral, "Stability Criterion for the Longitudinal Mode-Coupling Instability in the Presence of Both Space-Charge and Resonator Impedances", CERN/PS 2001-063 (AE).
- [24] G. Arduini et al., "Localizing Impedance Sources from Betatron Phase Beating in the CERN SPS", Proc. EPAC'04, Lucerne, Switzerland, 2004.
- [25] MAFIA, v.4.107, CST GmbH (Darmstadt, Germany), 2002; [www.cst.de](http://www.cst.de).
- [26] G. Rumolo et al., "Tracking Study of the Effect of BPM Impedances in the SPS", CERN-AB-2005-088-RF.

## APPENDIX A: MICROWAVE INSTABILITY WITH RF OFF

The unstable bunch spectrum when a single-bunch is injected into the SPS with RF OFF has been measured up to 2 GHz in 2001 and 2007 with similar beam parameters. The results are shown in Fig. A1. It can be seen that a resonance near 1.4 GHz, which was just visible in 2001, is clearly present in 2007.

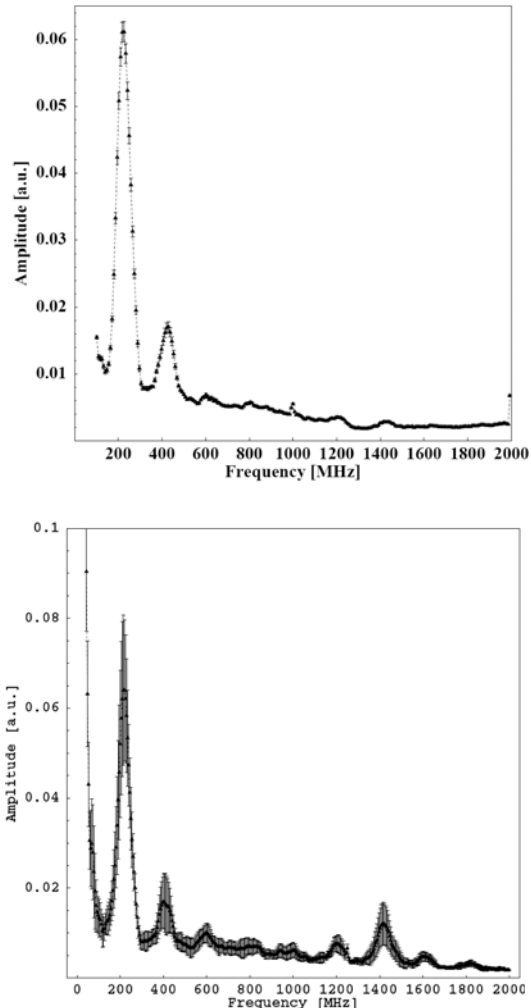


Figure A1: Unstable bunch spectra up to 2 GHz with RF OFF in 2001 (upper) and 2007 (lower), with similar beam parameters.

## APPENDIX B: LOCALIZED SPS IMPEDANCE FROM PHASE BEATING VS. INTENSITY

By detecting the current-dependent phase advance between adjacent Beam Position Monitors (BPMs) localized impedances around the ring could be identified in principle. This method is very attractive as it could help us to identify the remaining 13 M $\Omega$ /m of vertical “total” impedance, which for the moment are still

unknown. Measurements have been performed in 2007, but the data still have to be analyzed in detail, in particular to correctly take into account the effect of the detuning impedance. An example of what was obtained in 2003 is shown in Fig. B1 [24]. It was concluded that impedance is mainly concentrated in a few locations where the injection (MKP) kickers and extraction (MKE) kickers are, where the RF cavities are, and another location (in sextant 5) where the instrumentation is.

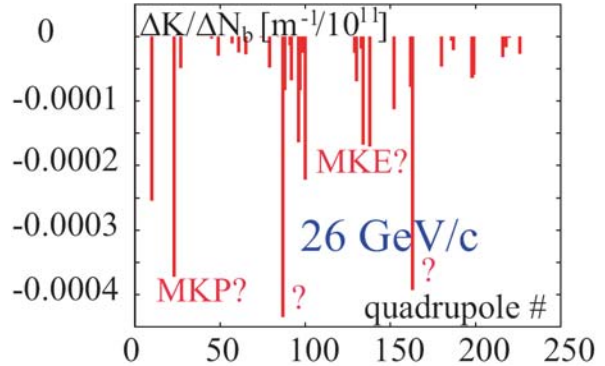


Figure B1: Local impedance distribution around the SPS ring from the measured current-dependent phase beating at 26 GeV/c in 2003.

## APPENDIX C: BEAM POSITION MONITORS

The impedance of the 108 horizontal beam position monitors (BPMH) and 108 vertical beam position monitors (BPMV) have been simulated with MAFIA [25]. The resulting longitudinal and vertical broad-band impedances (for all the BPMs) are  $\text{Im}[Z_x/n] = 0.02 \Omega$  and  $\text{Im}[Z_y] = 0.07 \text{ M}\Omega/\text{m}$  respectively, while the four most critical trapped modes (also for all the BPMs) are given in Table C1. It can be seen that the contribution of the BPMs to the broad-band impedance of the SPS machine is small. Furthermore, HEADTAIL simulations were performed with the four trapped modes and they revealed that the fast single-bunch vertical instability threshold was about one order of magnitude higher than the one measured [26]. The BPMs cannot therefore be held as the main responsible for the fast transverse instability observed in the SPS with low emittance bunches.

Table C1: Four most critical trapped modes for all the 108 horizontal and vertical beam position monitors (with the associated values of the betatron functions).

| $\beta_x$ [m] | $\beta_y$ [m] | $f_r$ [GHz] | $R_y$ [M $\Omega$ /m] | Q    |
|---------------|---------------|-------------|-----------------------|------|
| 103           | 21            | 0.537       | 500                   | 1951 |
| 103           | 21            | 1.836       | 254                   | 3367 |
| 22            | 101           | 0.786       | 180                   | 2366 |
| 22            | 101           | 2.270       | 222                   | 5880 |

## APPENDIX D: VACUUM PUMPING PORTS

The SPS machine comprises 216 main quadrupole magnets alternately focusing (QF) and defocusing (QD), in a classic FODO lattice, with a half cell length of 32 m. In the arcs, the space between the quadrupoles is occupied by 4 main bending magnets (MBA = dipole with large horizontal aperture and MBB = dipole with large vertical aperture) and a short straight section (SSS = Short Straight Section girder supporting BPM and correctors, together with, various multipole magnetic correction elements at different locations around the SPS).

Both longitudinal and transverse impedances of the (shielded) transitions [2,3] have been simulated with MAFIA. The resulting longitudinal and vertical broadband impedances for the 96 transitions QD\_MBB, 90 transitions MBB\_MBA, 90 transitions QF\_MBA, 180 transitions MBA\_MBA and 192 transitions MBB\_MBB (i.e. 648 transitions in total) are  $\text{Im}[Z_{\parallel}/n] = 0.02 \Omega$  and  $\text{Im}[Z_{\perp}] = 0.2 \text{ M}\Omega/\text{m}$  respectively, which are small compared to the measured values. The next step will consist to examine in detail the remaining kickers and septa which do not have shielded transitions.

## APPENDIX E: RF CAVITIES

There are four travelling-wave 200 MHz RF cavities, two with four sections and two with five sections, and each section is composed of 11 drift tubes. The real and imaginary parts of the (normalized) longitudinal impedance for all these cavities are plotted in Fig. E1. Due to the shape of the imaginary part of the impedance near 200 MHz, the effective impedance is very sensitive to the bunch length, as can be seen in Fig. E2. Over the last years measurements have been performed for total bunch lengths between  $\sim 2$  ns and  $\sim 3$  ns. It is seen from Fig. E2 that for a total bunch length of 3 ns the imaginary part of the effective (normalized) longitudinal impedance is higher than the one for a total bunch length of 2 ns by  $1.7 \Omega$ , which represents 23% of the measured impedance in 2006.

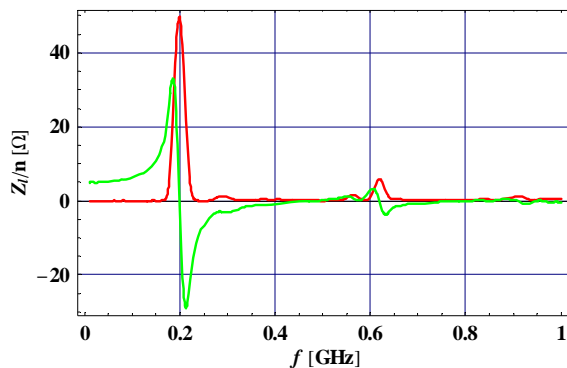


Figure E1: Real (red curve) and imaginary (green curve) parts of the longitudinal impedance vs. frequency for all the four travelling-wave 200 MHz RF cavities.

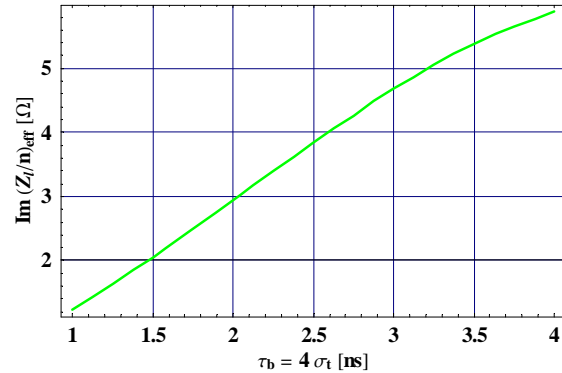


Figure E2: Imaginary part of the effective (normalized) longitudinal impedance vs. total bunch length  $\tau_b$  ( $4 \sigma_t$  Gaussian fit).

## APPENDIX F: HIGH ENERGY BEAM DUMP ABSORBER (TIDVG)

The TIDVG is the SPS high energy beam dump absorber with Graphite core installed in 1999. A titanium (Ti) coating of 1-2 microns was applied to the graphite blocks in order to prevent risk of polluting with graphite dust the downstream SPS injection kicker ( $\sim 7$  m downstream). As there was no high temperature treatment of the graphite applied, a poor condition of the graphite surface was obtained, which means that the Ti coating was very fragile. For this purpose, a Ti foil (with a thickness of  $\sim 50 \mu\text{m}$ ) was installed as an additional protection.

A visual inspection in March 2004 of the TIDVG (removed for LSS1 re-cabling) revealed a deformation of the Ti foil, which was traced back to be the reason for the limitation of the SPS vertical aperture.

During the 2007 run there was no Ti foil. Preliminary computations of the longitudinal resistive-wall impedance with or without the Ti foil revealed that the imaginary part of the effective (normalized) longitudinal impedance is much smaller than  $1 \Omega$ , and that the absence of the Ti foil in 2007 cannot be responsible for the measured increase.